Available online at www.sciencedirect.com
ScienceDirect
International Journal of Thermal Sciences 48 (2009) 154–164
International Journal of Thermal Sciences
www.elsevier.com/locate/ijts

Performance evaluation of a hybrid photovoltaic thermal (PV/T) (glass-to-glass) system

A.S. Joshi [a,b,1], A. Tiwari [a], G.N. Tiwari [a], I. Dincer [b,*], B.V. Reddy [b]

[a] *Centre for Energy Studies, Indian Institute of Technology-Delhi, Hauz Khas, New Delhi 110016, India*
[b] *Faculty of Engineering and Applied Science, University of Ontario Institute of Technology (UOIT), Oshawa, Ontario, Canada L1H 7K4*

Received 23 January 2008; received in revised form 30 April 2008; accepted 4 May 2008
Available online 3 June 2008

Abstract

In this paper, an attempt is made to evaluate the thermal performance of a hybrid photovoltaic thermal (PV/T) air collector system. The two type of photovoltaic (PV) module namely PV module with glass-to-tedlar and glass-to-glass are considered for performance comparison. The results of both PV modules are compared for composite climate of New Delhi. Analytical expression for solar cell, back surface, outlet air temperatures and an overall thermal efficiency are derived for both cases. It is observed that hybrid air collector with PV module glass-to-glass gives better performance in terms of overall thermal efficiency. Parametric studies are also carried out.

Keywords: PV module; Hybrid PV/T system; Thermal; Efficiency; Performance

1. Introduction

Energy is a key item in our relations with the environment. Energy consumption determines how much and how severely we can affect our environment, and how damaging or healing our interactions with it are. Its role is vital for our life and for our economy. Thermal form of energy also plays an important role in human's life as it can generally be utilized in the form of either high-grade (high-temperature) or low-grade (low-temperature). Solar photovoltaic and thermal applications appear to be one of the potential solutions for current energy needs and to combat greenhouse gas emissions.

Recently, Jones and Underwood [1] have studied the temperature profile of photovoltaic (PV) module in a non-steady state condition with respect to time. They performed experiments for clear as well cloudy day condition and observed that the PV module temperature varies between 300–325 K (27–52 °C) for an ambient air temperature of 297.5 K (∼ 24.5 °C). The thermal energy associated with PV module may either be removed (carried away) by air or water. When thermal energy requirement is integrated with photovoltaic (PV) module, it is referred to as hybrid PV/T system. Hybrid PV/T systems may find applications for: (i) air heating (e.g., [2–10]) and (ii) water heating (e.g., [9,11–17]).

Chow [14] has done the analysis of PV/T water collector with single glazing in a transient condition. The tube below flat plate with metallic bond collector was used. He observed that electrical efficiency is increased by 2% at mass flow rate of 0.01 kg/s for 10,000 $W/m^2\,K$ plate to bond heat transfer coefficient. An additional thermal efficiency of 60% was also observed. For water heating under natural mode of operation, Huang et al. [18] have studied experimentally the unglazed integrated photovoltaic and thermal solar system (IPVTS). They observed that the primary energy saving efficiency of IPVTS exceeds 0.60 which is higher than for a conventional solar water heater or pure PV system. Kalogirou [16] has studied the monthly performance of unglazed hybrid PV/T system under forced mode of operation for climatic condition of Cyprus and observed an increase of the mean annual efficiency of PV solar system from 2.8% to 7.7% with thermal efficiency of 49%, respectively. Similar study has also been carried out by Zondag et al. [17]. They have referred hybrid PV/T as a combi-panel

* Corresponding author.
E-mail address: ibrahim.dincer@uoit.ca (I. Dincer).
[1] Currently at UOIT as a Post-Doctoral Researcher.

1290-0729/$ – see front matter
doi:10.1016/j.ijthermalsci.2008.05.001

Nomenclature

A	Area of PV module	m^2
A_c	Area of solar cell	m^2
b	Breadth of PV module	m
C_a	Specific heat of air	kJ/kg K
C_f	Conversion factor of the thermal power plant	
dx	Elemental length	m
e	Root mean square of percentage deviation	%
EVA	Ethyl Vinyl Acrelate	
G	Subscript for glass to glass PV/T system	
h_{ba}	Heat transfer coefficient from black surface to air	W/m^2 K
h_t	Heat transfer coefficient from back surface to air through glass	W/m^2 K
h_T	Heat transfer coefficient from back surface to air through tedlar	W/m^2 K
h_{p1G}	Penalty factor due to presence of solar cell material, glass and EVA for glass to glass PV/T system	
h_{p1T}	Penalty factor due to presence of solar cell material, glass and EVA for glass to tedlar PV/T system	
h_{p2G}	Penalty factor due to presence of interface between glass and working fluid through absorber plate for glass to glass PV/T system	
h_{p2T}	Penalty factor due to presence of interface between tedlar and working fluid through absorber plate for glass to tedlar PV/T system	
I_{max}	Maximum current	A
I_{sc}	Short circuit current	A
$I(t)$	Incident solar intensity (a function of time) on the inclined module surface	W/m^2
k_T	Conductive heat transfer coefficient from solar cell to back surface	W/m^2 K
L	Length of the PV module	m
M	Time	hour
$\dot{m}_a$	Rate of flow of air mass	kg/s
N	Number of experimental/predicted data	
PV	Photovoltaic	
PV/T	Photovoltaic thermal	
$\dot{Q}$	Rate of useful energy	W
r	Linear coefficient of correlation (dimensionless)	
T	Subscript for glass to tedlar PV/T system	
T_a	Ambient air temperature	°C
T_{air}	Flowing air temperature inside the duct above back surface	°C
$T_{air\,in}$	Inlet air temperature	°C
$T_{air\,out}$	Outlet air temperature	°C
T_{bs}	Back surface temperature of tedlar	°C
T_c	Temperature of solar cell	°C
U_b	Overall heat transfer coefficient from bottom to ambient	W/m^2 K
U_L	Overall heat transfer coefficient from solar cell to ambient through top and back surface of insulation	W/m^2 K
U_t	Overall heat transfer coefficient from solar cell to ambient through glass cover	W/m^2 K
U_{tb}	Overall heat transfer coefficient from glass to black surface through solar cell	W/m^2 K
U_{tT}	Overall heat transfer coefficient from tedlar to back surface through solar cell	W/m^2 K
V_{max}	Maximum voltage	Volt
V_{oc}	Open circuit voltage	Volt
v	Duct air velocity	m/s
X_{exp}	Experimental data	
X_{pre}	Predicted or theoretical data	

Greek Letters

α_c	Absorptivity of solar cell	
α_b	Absorptivity of black surface	
β_c	Packing factor of solar cell	
η_c	Solar cell efficiency	%
η_E	Electrical efficiency	%
η_{Eth}	Thermal efficiency equivalent of electrical efficiency	%
η_o	Overall thermal efficiency	%
η_{th}	Thermal efficiency	%
τ_g	Transitivity of glass	

that converts solar energy into both electrical and thermal energy. The electrical and thermal efficiency of combi-panel were reported as 6.7% and 33%, respectively.

Sandnes and Rekstad [12] have observed the behavior of a combined photovoltaic/ thermal (PV/T) collector which was constructed by pasting single-crystal silicon cells onto a black plastic solar heat absorber (unglazed PV/T system). They recommended that the combined PV/T concept must be used for low temperature thermal application for increasing the electrical efficiency of PV system, e.g., space heating of a building. Zakharchenko et al. [13] have also studied unglazed hybrid PV-thermal system with a suitable thermal contact between the panel and the collector. They have proved that the areas of PV panel and collector in PV/T system need not be equal for higher overall efficiency. To operate PV module at low temperature, PV module should cover the low temperature part of the collector (at cold water inlet portion). Further, unglazed hybrid photovoltaic/thermal with booster diffuse reflector was integrated with horizontal roof of a building by Tripanagnostopoulos et al. [9]. They suggested that PV/T system with reflector gives clearly higher electrical and thermal output. They have also studied the performance characteristic of PV/water and PV/air systems. Infield et al. [8] have derived an overall heat loss coefficient (U) and thermal energy gain factor (g) for ventilated vertical photovoltaic (PV) module and double glazed window (PV facades). The steady state analysis was used to determine ventilation gains and transmission losses in terms of irradiation (solar radiation) and various heat transfer processes involved in facades. He observed that the ventilated facades ensure that the electrical efficiency of PV module is improved due to low temperature (generally below 45 °C). Hegazy and Sopian et al. [7,19] investigated glazed photovoltaic/thermal air (PV/T air) system for single and double pass air heater for space heating and drying purposes. They have also developed a thermal model for each system. They observed that thermal energy for glazed PV/T system has increased with lower electrical efficiency due to high operating temperature. Further, Coventry [20] has studied the performance of a concentrating photovoltaic/thermal solar collector and concluded that an overall thermal and electrical efficiency of PV/T concentrating system are 58% and 11%, respectively. This gives a total efficiency of the system as 69%.

Sahin et al. [21] has recently investigated the thermodynamic characteristics of solar photovoltaic (PV) cells from a perspective based on exergy. They found the energy efficiency of a solar cell varies between 7% and 12% and exergy efficiency, which incorporates the second law of thermodynamics and account for solar irradiation exergy, varies between 2% and 8%.

In this paper, it is aimed to study the performance of unglazed hybrid photovoltaic thermal (PV/T) glass-to-glass system for composite climate of New Delhi and the comparison with glass-to-tedlar (PV/T) system. An experimental validation of Tiwari et al. [3] is also carried out in terms of various temperatures, e.g., back surface temperature, cell temperature and outlet air temperature. The comparison of both the systems is done in terms of various temperatures, e.g., back surface temperature, cell temperature and outlet air temperature and thermal, overall thermal and electrical efficiencies. Furthermore, the variation of overall thermal efficiency with length of collector and different duct air velocities is studied for both models.

2. General terms for analysis

Various terms used to evaluate thermal performance of a hybrid photovoltaic thermal (PV/T) glass-to-glass system are discussed below:

• Solar cell:
Solar cell is a device that converts sunlight to electricity using photovoltaic effect. It is also called as Photovoltaic (PV) cell. The initials PV stand for photo (light) and voltaic (electricity). The basic phenomenon was discovered in the 19th century. The Photovoltaic cells were significantly developed at Bell Labs in 1950, primarily for space applications.

• Short circuit current (I_{sc}):
The solar cell generates a current, and this current varies with the cell voltage. When the voltage of this solar cell is zero-described as a 'short-circuited' solar cell—the short circuit current, I_{sc}, proportional to irradiance on the solar cell, can be measured [22]. In other words, the short circuit current is the current for no voltage in the solar cell circuit. This can be achieved by connecting the positive and negative terminals by copper wire.

• Open circuit voltage (V_{oc}):
When the cell current is equal to zero, the solar cell is described as 'open-circuited'. The cell voltage then becomes the open circuit voltage (V_{oc}).

• Fill factor (FF):
The fill factor is defined as follows:

$$FF = \frac{I_{max} \times V_{max}}{I_{sc} \times V_{oc}} \tag{1}$$

• Efficiency of a solar cell (η_c):
The efficiency of a solar cell can be given as

$$\eta_c = \frac{I_{max} \times V_{max}}{A_c \times I(t)} \tag{2}$$

where I_{max} and V_{max} are the current and voltage for maximum power, corresponding to solar intensity, $I(t)$.

The specifications of the silicon solar cell, as provided by the manufacturer [23] at 1000 W/m^2 at 25 °C (standard test conditions) used in the PV module are as follows:

- Fill factor (FF) = 0.72
- Short circuit current (I_{sc}) = 4.8 A
- Open circuit voltage (V_{oc}) = 21.7 V
- Area of single solar cell (A_c) = 0.0139 m^2
- Efficiency of solar cell (η_c) = 15%

• Photovoltaic (PV) module:
The photovoltaic module consists of 36 solar cells connected in series. Each solar cell has an effective area of 0.0139 m^2. Area of one PV module (A) is 0.605 m^2. The efficiency of a PV module (η_E) is less than the efficiency of solar cell (η_c) due to ohmic loss occurring between the two solar cells connected in series and the packing factor (< 1). Due to the more energy payback period of a photovoltaic (PV) module, the cost of electricity produced by a PV module is higher than that of electricity produced by fossil fuels. In order to reduce the energy payback period, a PV module can also be used for thermal applications such as air/water heating, space heating, solar agricultural drying; it can then be more cost effective. Such systems are referred to as hybrid photovoltaic thermal systems. Design parameters for hybrid photovoltaic thermal system with air as the heat removal medium has been given in Table 1.

Table 1
Design parameters for hybrid photovoltaic thermal system with air as the heat removal medium

Parameters	Values	Parameters	Values
A	0.605 m^2	U_b	0.62 W/m^2 K
b	0.45 m	U_t	2.8 W/m^2 K
h_{p1}	0.88	h_T	6.5 W/m^2 K
L	1.2 m	U_{tT}	8.11 W/m^2 K
β_c	0.83	U_T	66 W/m^2 K
η_c	0.12	α_c	0.90
τ_g	0.95	α_T	0.50

3. System description

A schematic view of a photovoltaic thermal air collector is shown in Fig. 1(a). A parallel flat plate air duct is provided below the glass base of a solar cell. The different components of a photovoltaic thermal air collector are clearly indicated in the same figure. When solar radiations fall on the solar cells of PV module, it gets converted into electricity and heat. The electrical energy is stored in a battery. Due to the thermal energy of the solar radiation the PV modules get heated. Solar cells made up of electronic circuits loose its efficiency when heated. In order to maintain a good electrical efficiency of the system the heat removal from the PV panel is essential. Therefore the thermal energy available on the back surface of the PV module is carried away by blowing air below the PV module by using DC fans. These DC fans consume a small amount of electricity from the battery itself which is neglected in the present study. The different temperature measurements such as inlet air temperature, solar cell temperature, back surface temperature, outlet air temperature and ambient temperature are carried out by using the digital temperature indicators as shown in the same figure. All the temperature measurements are done with the calibrated thermocouples or thermometers to ensure the accuracy. The global and diffuse radiations in W/m^2 are measured by using a pyranometer. To ensure the accuracy of global radiation measurement, uncertainty analysis is necessary. The internal estimate of uncertainty is inherent in the data itself and its quantitative assessment is termed as the internal estimate of uncertainty. This occurs because an instrument may indicate a slightly different value every time a given input is fed to an instrument. In other words, one may say that the data is associated with scatter in values. The internal estimate uncertainty is also termed as internal standard error of uncertainty or internal standard error. The uncertainty analysis of measured global radiation for Solar Energy Park, IIT Delhi is done and the internal estimate of uncertainty is evaluated following Joshi [24] and it is found that the value for uncertainty for the measured global radiation is 9.62% (for further details, see Joshi [24]).

Digital clamp meter is used to measure the various currents (e.g., short circuit current, battery current, etc.) in Ampere and voltages (e.g., battery voltage, open circuit voltage, etc.) in Volt. Digital anemometer is used to measure the air flow in m/s at different locations, i.e., air entering and leaving the duct. The duct air velocity is calculated by taking the average of inlet and outlet air flow. The experimental observations of hybrid photovoltaic thermal PV/T air collector for the month of May at Solar Energy Park, IIT Delhi are given in Table 2. The photograph of the experimental set up is shown in Fig. 1(b).

In this paper, two types of PV module are considered for analysis and performance investigation:

- Case 1: PV module with glass-to-tedlar as shown in Fig. 2(a). In this case, solar radiation is absorbed by solar cell and EVA and it is then conducted to base of the tedlar for thermal heating of air flowing below tedlar as shown in Fig. 2(a).

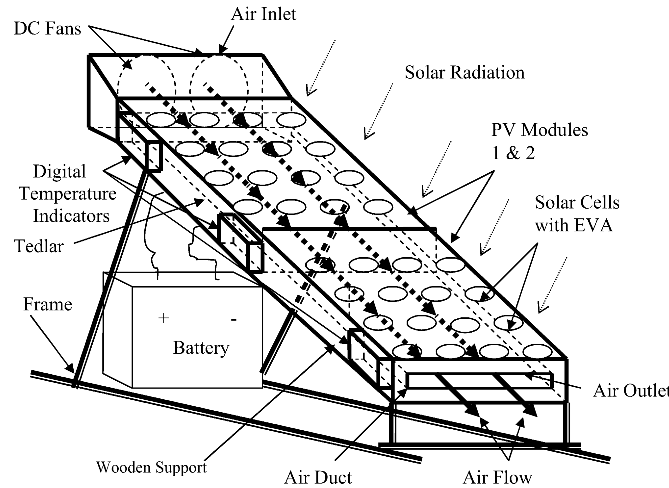

(a)

(b)

Fig. 1. (a) Schematic diagram of hybrid PV/T air collector. (b) Photograph of experimental setup of hybrid PV/T air collector at IIT Delhi.

- Case 2: PV module with glass-to-glass as shown in Fig. 2(b). In this case, solar radiation is absorbed by solar cell and black surface of insulating base and the flowing air is heated by convective heat from black surface as well as heat conducted from solar cell thorough glass cover below solar cell as shown in Fig. 2(b).

A part of solar energy is converted into the electricity and the rest into thermal energy, available from the black surface. The air is considered as a working fluid in all analyses.

Table 2
Experimental observation of hybrid photovoltaic thermal PV/T air collector for the month of May at Solar Energy Park, IIT Delhi

Time (hour)	Solar radiation (W/m^2)	Open circuit voltage (V)	Short circuit current (A)	Inlet air temperature (°C)	Back surface temperature (°C)	Solar cell temperature (°C)	Outlet air temperature (°C)	Ambient air temperature (°C)	Duct air velocity (m/s)
8 am	313.63	19.30	3.30	31.9	37.90	37.60	33.20	29.00	2.67
9 am	409.63	19.20	4.20	33.0	42.90	41.40	36.30	30.00	1.98
10 am	535.50	19.10	5.80	34.9	46.80	47.90	38.90	32.00	1.42
11 am	634.25	18.70	6.10	36.2	51.00	50.40	41.70	35.00	1.87
12 pm	658.00	18.40	6.50	42.3	57.20	54.90	46.10	38.00	1.73
1 pm	594.25	18.20	5.90	43.7	37.20	54.70	41.50	40.00	1.67
2 pm	558.00	18.30	4.60	42.0	54.90	52.90	46.40	41.00	1.77
3 pm	416.13	18.40	3.60	41.4	48.60	50.70	44.50	41.00	1.70
4 pm	253.75	18.30	2.60	40.8	46.40	47.20	43.00	40.00	1.83
5 pm	108.50	18.10	1.40	39.0	41.80	42.30	40.30	39.00	1.77

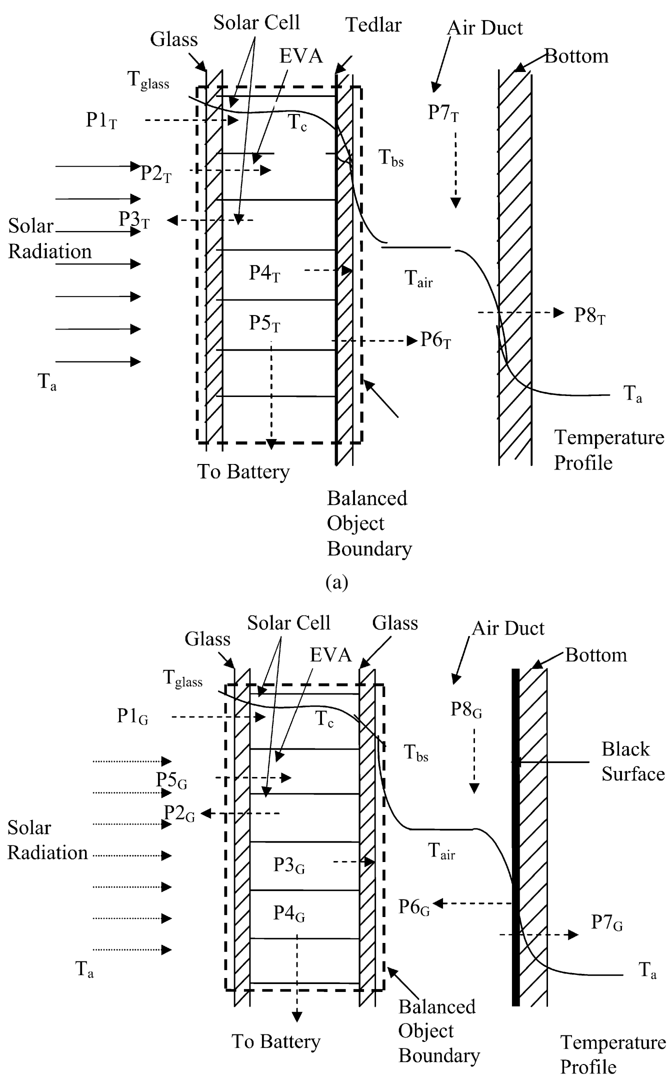

Fig. 2. (a) A cross-sectional view of glass-to-tedlar hybrid PV/T air collector. (b) A cross-sectional view of glass-to-glass hybrid PV/T air collector.

4. Energy analysis of the hybrid PV/T air collector

Following assumptions are made in order to write the energy balance equation for each component of a PV/T air collector system:

- The system is in quasi-steady state condition.
- The transmittivity of EVA is nearly 100%.
- The temperature variation along the thickness is negligible.
- The airflow through duct is uniform for the forced mode of operation for streamline flow.

Two cases are discussed as glass-to-tedlar (Fig. 2(a)) and glass-to-glass (Fig. 2(b)). Following Tiwari et al. [3] and Joshi [24], the energy balance equations for each component in watts are:

- For the PV module:

Case 1: For glass to tedlar PV module:

$$P1_T\,dA + P2_T\,dA = P3_T\,dA + P4_T\,dA + P5_T\,dA \tag{3a}$$

where $dA = b\,dx =$ the elemental area, $P =$ parameter and $T =$ subscript for glass to tedlar.

This equation can further be simplified as

$$P1_T + P2_T = P3_T + P4_T + P5_T$$

where $P1_T = \tau_g\alpha_c I(t)\beta_c =$ the rate of solar energy received by solar cell after transmission, $P2_T = \tau_g(1-\beta_c)\alpha_T I(t) =$ the rate of solar energy absorbed by tedlar after transmission from EVA, $P3_T = U_t(T_c - T_a) =$ the rate of heat loss from solar cell to ambient through glass cover, $P4_T = k_T(T_c - T_{bs}) =$ the rate of heat transfer from solar cell to back surface, and $P5_T = \eta_c I(t)\beta_c\tau_g =$ the rate of electrical energy available from solar cell of PV module.

Case 2: For glass to glass PV module:

$$P1_G\,dA = P2_G\,dA + P3_G\,dA + P4_G\,dA \tag{3b}$$

where $G =$ subscript for glass to glass PV/T system.

This equation can further be simplified as

$$P1_G = P2_G + P3_G + P4_G$$

where $P1_G = \tau_g\alpha_c I(t)\beta_c =$ the rate of solar energy received by solar cell after transmission, $P2_G = U_t(T_c - T_a) =$ the rate of heat loss from solar cell to ambient through glass cover, $P3_G = h_t(T_c - T_{bs}) =$ the rate of heat transfer from solar cell to back surface, and $P4_G = \eta_c I(t)\beta_c\tau_g =$ the rate of electrical energy available from solar cell of PV module.

- For the back surface:

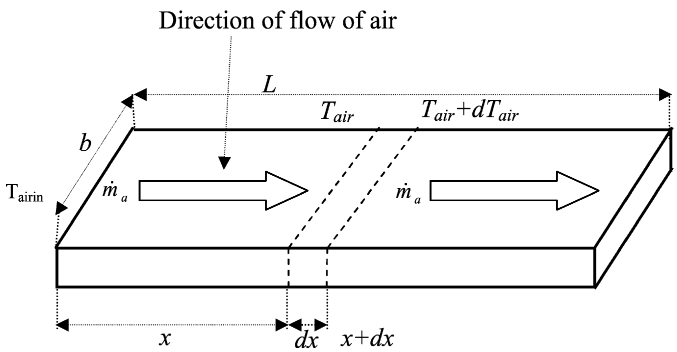

Fig. 3. An elemental length 'dx' shows the flow pattern of air.

Case 1: For glass to tedlar PV module:
Energy balance for back surface of the tedlar is as follows:

$$P4_T\,dA = P6_T\,dA \tag{4a}$$

This equation can be simplified to

$$P4_T = P6_T$$

where $P6_T = h_T(T_{bs} - T_{\text{air}})$ = the rate of heat transfer from back surface to flowing air.

Case 2: For glass to glass PV module:
Energy balance for back surface is as follows:

$$P5_G\,dA + P3_G\,dA = P6_G\,dA + P7_G\,dA \tag{4b}$$

After cancelling the common terms, the equation becomes

$$P5_G + P3_G = P6_G + P7_G$$

where $P5_G = \alpha_b\tau_g^2(1-\beta_c)I(t)$ = the rate of solar energy absorbed by black surface after transmission from EVA, $P6_G = h_{ba}(T_{bs} - T_{\text{air}})$ = the rate of heat transfer from black surface to flowing air, and $P7_G = U_b(T_{\text{air}} - T_a)$ = the rate of heat loss from flowing air to ambient air though insulation.

- For air flowing through air duct (Fig. 3):

Case 1: For glass to tedlar PV module:
For the air flowing below the Tedlar (air duct):

$$P6_T\,dA = P7_T\,dA + P8_T\,dA \tag{5a}$$

The above equation can also be written as

$$P6_T = P7_T + P8_T$$

where $P7_T = \dot{m}_a C_a \frac{dT_{\text{air}}}{dx}\,dx$ = the heat carried away with the flowing air and $P8_T = U_b(T_{\text{air}} - T_a)$ = the rate of heat loss from flowing air to ambient through insulation.

Case 2: For glass to glass PV module:

$$P6_G\,dA = P7_G\,dA + P8_G\,dA \tag{5b}$$

Simplifying above equation, we get

$$P6_G = P7_G + P8_G$$

where $P8_G = \dot{m}_a C_a \frac{dT_{\text{air}}}{dx}\,dx$ = the heat carried away with the flowing air.

From Eq. (3), an expression for the solar cell temperature in the terms of the back surface temperature of the PV module and climate parameters is obtained as:

Case 1: For glass to tedlar PV module:

$$T_c = \frac{\tau_g\beta_c I(t)(\alpha_c - \eta_c - \alpha_T(1-\frac{1}{\beta_c})) + U_t T_a + h_T T_{bs}}{U_t + h_T} \tag{6a}$$

Case 2: For glass to glass PV module:

$$T_c = \frac{\tau_g\beta_c I(t)(\alpha_c - \eta_c) + U_t T_a + h_t T_{bs}}{U_t + h_t} \tag{6b}$$

By substituting T_c from Eq. (6) in Eq. (4), we can obtain an expression for the back surface temperature of a PV module as:

Case 1: For glass to tedlar PV module:

$$T_{bs} = \frac{h_{P1T}(\alpha\tau)_{\text{eff}\,T} I(t) + U_{tT} T_a + h_T T_{\text{air}}}{h_T + U_{tT}} \tag{7a}$$

where,

$$(\alpha\tau)_{\text{eff}\,T} = \tau_g\beta_c\left(\alpha_c - \eta_c - \alpha_T\left(1 - \frac{1}{\beta_c}\right)\right) \quad \text{and}$$

$$h_{p1T} = \frac{h_T}{U_t + h_T}$$

is the penalty factor due to the glass cover of a PV module.

Case 2: For glass to glass PV module:

$$T_{bs} = \frac{(\alpha\tau)_{\text{eff}\,G} I(t) + (U_b + U_{tb})T_a + h_{ba} T_{\text{air}}}{h_{ba} + U_{tb} + U_b} \tag{7b}$$

By substituting T_c and T_{bs} of Eqs. (6) and (7) respectively in Eq. (5), we get

Case 1: For glass to tedlar PV module:

$$\frac{dT_{\text{air}}}{dx} + \left(\frac{bU_L}{\dot{m}_a C_a}\right)(T_{\text{air}} - T_a) = \frac{b h_{p1T} h_{p2T} (\alpha\tau)_{\text{eff}\,T} I(t)}{\dot{m}_a C_a} \tag{8a}$$

where $U_L = (U_b + U_{t\text{air}})$ and $h_{p2T} = h_T/(U_{tT} + h_T)$ is the penalty factor due to the presence of tedlar.

Case 2: For glass to glass PV module:

$$\frac{dT_{\text{air}}}{dx} + \left(\frac{bU_L}{\dot{m}_a C_a}\right)(T_{\text{air}} - T_a) = \frac{b h_{p2G} (\alpha\tau)_{\text{eff}\,G} I(t)}{\dot{m}_a C_a} \tag{8b}$$

where $U_L = h_{p2G}(U_b + U_{tb})$ and $h_{p1G} = h_t/(U_t + h_t)$ is the penalty factor due to the glass cover of a PV module, and $h_{p2G} = h_{ba}/(h_{ba} + U_b + U_{tb})$, is the penalty factor due to the presence of black surface, further $(\alpha\tau)_{\text{eff}\,G} = \alpha_b\tau_g^2(1-\beta_c) + h_{p1G}(\tau_g\beta_c(\alpha_c - \eta_c))$.

By integrating Eq. (8) with the initial condition $T_{\text{air}} = T_{\text{air}\,\text{in}}$, at $x = 0$ we get an expression for the temperature of the flowing air inside the air duct as:

Case 1: For glass to tedlar PV module:

$$T_{\text{air}} = \left[T_a + \frac{h_{p1T} h_{p2T} (\alpha\tau)_{\text{eff}\,T} I(t)}{U_L}\right]\left(1 - e^{-bU_L x/(\dot{m}_a C_a)}\right) + T_{\text{air}\,\text{in}} e^{-bU_L x/(\dot{m}_a C_a)} \tag{9a}$$

Case 2: For glass to glass PV module:

$$T_{\text{air}} = \left[T_a + \frac{h_{p2G} (\alpha\tau)_{\text{eff}\,G} I(t)}{U_L}\right]\left(1 - e^{-bU_L x/(\dot{m}_a C_a)}\right) + T_{\text{air}\,\text{in}} e^{-bU_L x/(\dot{m}_a C_a)} \tag{9b}$$

The outlet air temperature ($T_{\text{air out}}$) of the flowing air inside the air duct can be obtained from Eq. (9) for two cases.

Case 1: For glass to tedlar PV module:

$$T_{\text{air out}} = \left[T_a + \frac{h_{p1T} h_{p2T} (\alpha\tau)_{\text{eff}\,T} I(t)}{U_L}\right]\left(1 - e^{-bU_L L/(\dot{m}_a C_a)}\right) + T_{\text{air in}} e^{-bU_L L/(\dot{m}_a C_a)} \tag{10a}$$

Case 2: For glass to glass PV module:

$$T_{\text{air out}} = \left[T_a + \frac{h_{p2G} (\alpha\tau)_{\text{eff}\,G} I(t)}{U_L}\right]\left(1 - e^{-bU_L L/(\dot{m}_a C_a)}\right) + T_{\text{air in}} e^{-bU_L L/(\dot{m}_a C_a)} \tag{10b}$$

The average air temperature of the flowing air above the black surface over the length of air duct below the PV module is obtained as:

Case 1: For glass to tedlar PV module:

$$\bar{T}_{\text{air}} = \left[T_a + \frac{h_{p1T} h_{p2T} (\alpha\tau)_{\text{eff}\,T} I(t)}{U_L}\right] \times \left[1 - \left(\frac{1 - e^{-bU_L L/(\dot{m}_a C_a)}}{bU_L L/(\dot{m}_a C_a)}\right)\right] + T_{\text{air in}} \left(\frac{1 - e^{-bU_L L/(\dot{m}_a C_a)}}{bU_L L/(\dot{m}_a C_a)}\right) \tag{11a}$$

Case 2: For glass to glass PV module:

$$\bar{T}_{\text{air}} = \left[T_a + \frac{h_{p2G} (\alpha\tau)_{\text{eff}\,G} I(t)}{U_L}\right]\left[1 - \left(\frac{1 - e^{-bU_L L/(\dot{m}_a C_a)}}{bU_L L/(\dot{m}_a C_a)}\right)\right] + T_{\text{air in}} \left(\frac{1 - e^{-bU_L L}/(\dot{m}_a C_a)}{bU_L L/(\dot{m}_a C_a)}\right) \tag{11b}$$

After determining the average air temperature of the flowing air inside the air duct form the above equation, the black surface temperature of a PV module can be obtained from Eq. (7). Then we can evaluate solar cell temperature for given climate parameters of a solar intensity and ambient air temperature:

The rate of useful thermal energy obtained from the PV/T air collector is thus obtained for two cases.

Case 1: For glass to tedlar PV module:

$$\dot{Q} = \frac{\dot{m}_a C_a}{U_L}\left[h_{p1T} h_{p2T} (\alpha\tau)_{\text{eff}\,T} I(t) - U_L (T_{\text{air in}} - T_a)\right]\left(1 - e^{-bU_L L/(\dot{m}_a C_a)}\right) \tag{12a}$$

Case 2: For glass to glass PV module:

$$\dot{Q} = \frac{\dot{m}_a C_a}{U_L}\left[h_{p2G} (\alpha\tau)_{\text{eff}\,G} I(t) - U_L (T_{\text{air in}} - T_a)\right]\left(1 - e^{-bU_L L/(\dot{m}_a C_a)}\right) \tag{12b}$$

The thermal efficiency of the PV/T collector is

$$\eta_{\text{th}} = \frac{\sum_{i=1}^{M} \dot{Q}}{\sum_{i=1}^{M} I(t) bL} \tag{13}$$

where M is time in hour.

The electrical efficiency of the PV/T collector can be given as [17]

$$\eta_E = \eta_c\left[1 - 0.0045(\bar{T}_c - 25)\right] \tag{14}$$

Here we convert the conventional electrical efficiency to thermal efficiency equivalent through the following equation:

$$\eta_{E\text{th}} = \frac{\eta_E}{C_f} \tag{15}$$

where C_f is the conversion factor of the thermal power plant and its value may be taken as 0.36 for countries like India [25].

The overall thermal efficiency of the PV/T collector can be calculated by adding the thermal efficiency (Eq. (13)) and thermal efficiency equivalent of electrical efficiency (Eq. (15)) as

$$\eta_o = (\eta_E / C_f) + \eta_{\text{th}} \tag{16}$$

- Root mean square of percentage deviation (e) and linear coefficient of correlation (r)

Furthermore, the root mean square of percentage deviation (e) and linear coefficient of correlation (r) are evaluated by using the following expressions:

$$e = \sqrt{\frac{\sum (e_i)^2}{n}} \tag{17}$$

where,

$$e_i = \left[\frac{X_{\text{pre}(i)} - X_{\exp(i)}}{X_{\text{pre}(i)}}\right] \times 100$$

and

$$r = \frac{N\left(\sum X_{\exp} \cdot X_{\text{pre}}\right) - \left(\sum X_{\exp}\right) \cdot \left(\sum X_{\text{pre}}\right)}{\sqrt{N \cdot \left(\sum X_{\exp}^2\right) - \left(\sum X_{\exp}\right)^2} \cdot \sqrt{N . \left(\sum X_{\text{pre}}^2\right) - \left(\sum X_{\text{pre}}\right)^2}} \tag{18}$$

The linear coefficient of correlation ranges between −1 and 1, measures the strength and the direction of a linear relationship between two variables, i.e., the experimental and theoretical/predicted values. The experimental and theoretical/predicted values are said to be in a strong positive linear correlation, if 'r' is close to 1. The values of 'e' and 'r' for the reproduced data are shown in respective figures in the following section.

5. Results and discussion

In glass-to-glass PV/T air collector, absorber plate (blackened surface) is used in place of tedlar. In this case, more radiations transmitted from glass get absorbed on the black surface as compared to tedlar surface. Hence more thermal energy is available on the black surface. By using a fan this thermal energy can be removed and used for various purposes like space heating, air heating, water heating, solar agricultural/crop drying, etc. After thermal modeling one can see the differences between two cases in rate of useful thermal energy by comparing the various parameters of Eqs. (12). The comparisons of various parameters of Eqs. (12) are given in Table 3. It can be

Table 3
Comparison of the glass to tedlar and glass to glass PV/T air collectors

PV/T air collector	Packing factor (glass cover)	Packing factor (tedlar/glass)	Product of packing factors	Useful thermal energy
Glass to tedlar	$h_{p1T} = 0.8988$	$h_{p2T} = 0.2154$	$h_{p1T} h_{p2T} (\alpha\tau)_{\mathrm{eff}\,T} = 0.1347$	$\dot{Q} = \frac{\dot{m}_a C_a}{U_L}\left[h_{p1T} h_{p2T} (\alpha\tau)_{\mathrm{eff}\,T} I(t) - U_L(T_{\mathrm{air\,in}} - T_a)\right]\left(1 - e^{-bU_L L/(\dot{m}_a C_a)}\right)$
Glass to glass	$h_{p1G} = 0.9782$	$h_{p2G} = 0.1890$	$h_{p2G} (\alpha\tau)_{\mathrm{eff}\,G} = 0.1418$	$\dot{Q} = \frac{\dot{m}_a C_a}{U_L}\left[h_{p2G} (\alpha\tau)_{\mathrm{eff}\,G} I(t) - U_L(T_{\mathrm{air\,in}} - T_a)\right]\left(1 - e^{-bU_L L/(\dot{m}_a C_a)}\right)$

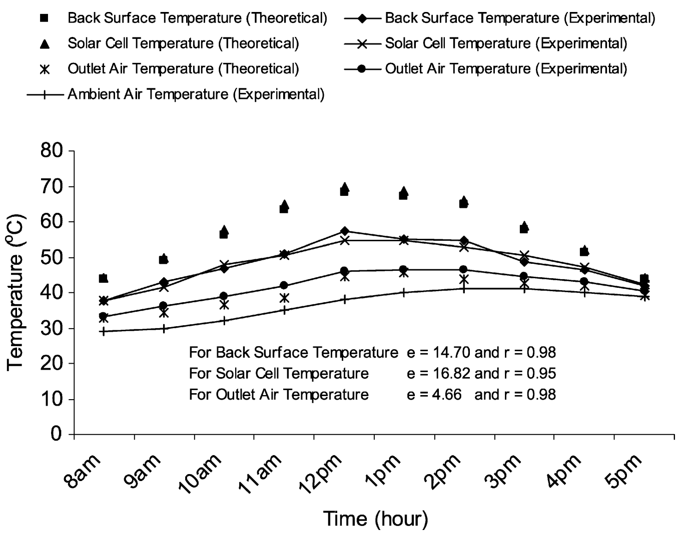

Fig. 4. Experimental validation of hourly variation of back surface, solar cell and outlet air temperature for glass-to-tedlar hybrid PV/T air collector.

seen from Table 3 that rate of useful thermal energy is more in case of glass-to-glass PV/T air collector.

Experiments were carried out for the hybrid PV/T glass-to-tedlar air collector for the month of May at Solar Energy Park, IIT Delhi. Table 2 shows the observed values of solar intensity, ambient air temperature, inlet air temperature, back surface temperature, solar cell temperature, outlet air temperature, short circuit current, open circuit voltage and duct air velocity with time for the forced mode of operation with air flow with single fan for the month of May for New Delhi. Using the data of Table 2 and following Tiwari et al. [3] and Joshi [24], back surface temperature, solar cell temperature, outlet air temperature, electrical efficiency, thermal efficiency and overall thermal efficiency, are calculated for glass-to-tedlar PV/T air collector. Fig. 4 shows the experimental validation of hourly variation of back surface, solar cell and outlet air temperature for glass-to-tedlar PV/T air collector. The root mean square deviation (e) and linear coefficient of correlation (r) are calculated by using Eqs. (17) and (18), respectively. It is found that there is a fair agreement between the experimental and the theoretical results with a mean square deviation 'e' $= 5$–17% and the value of linear coefficient of regression 'r' $= 0.95$–0.98. The outlet air temperature varies from a minimum value of 33 °C at 8 am to a maximum of 46 °C at 12 pm. The back surface and solar cell vary from a minimum value of 38 °C at 8 am to a maximum of 57 and 55 °C respectively at 12 pm. The theoretical values for back surface and solar cell temperatures are slightly higher then the experimental values and ranging between a minimum value of 43 °C at 8 am and a maximum of 67 °C at 12 pm

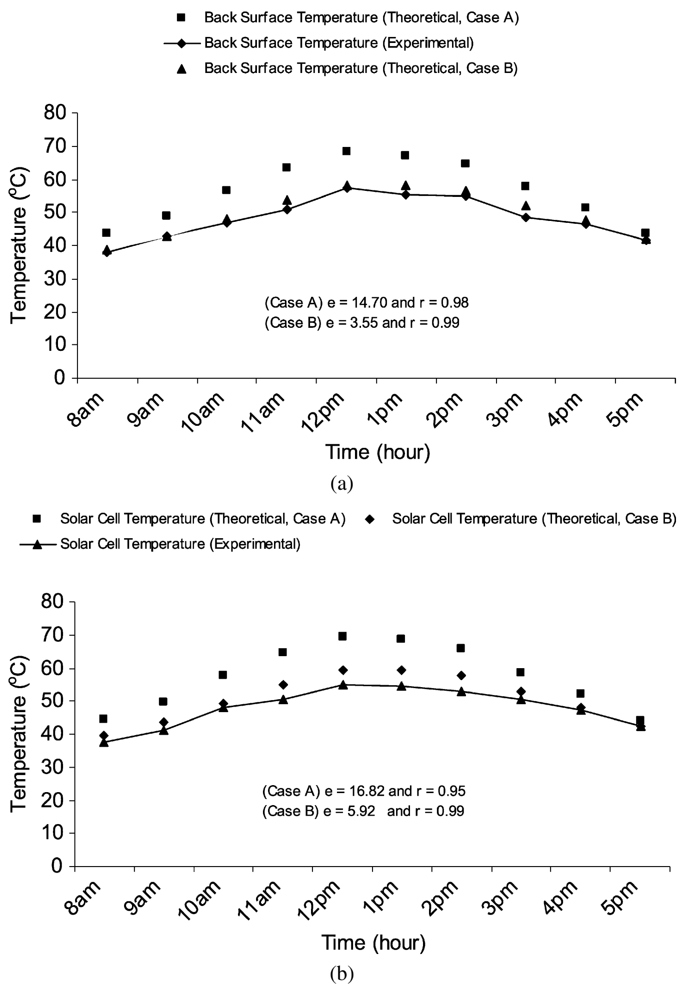

Fig. 5. (a) Comparison of experimental and theoretical back surface temperature (Cases A, B). (b) Comparison of experimental and theoretical solar cell temperature (Cases A, B).

for both. However the agreement in the theoretical and experimental values of back surface and solar cell temperatures is closer for higher duct air velocity (3.2 m/s) (Case A) which is shown in Figs. 5. In Case B, the duct air velocity is kept at a value of 1.6 m/s. Figs. 5(a) and 5(b) respectively show a closer agreement for the back surface temperature with $e = 3.6\%$ and $r = 0.99$ and solar cell temperature with $e = 6\%$ and $r = 0.99$ for Case B. Fig. 6 shows the hourly variation of electrical, thermal and overall thermal efficiency for glass-to-tedlar PV/T air collector. The electrical efficiency ranges between 10–11% through out the day where as thermal efficiency ranges between 13–16.5%. The overall thermal efficiency is of the order of 41–45.4%. In order to calculate overall thermal efficiency,

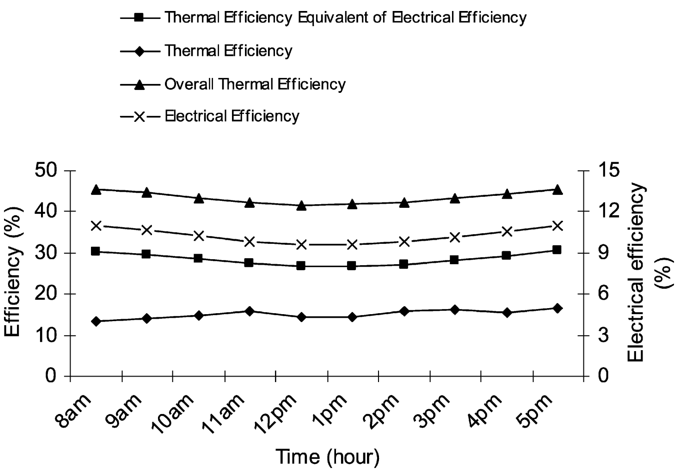

Fig. 6. Hourly variation of thermal, electrical and overall thermal efficiencies for glass-to-tedlar hybrid PV/T air collector.

first the electrical efficiency is converted into equivalent thermal efficiency and then added to thermal efficiency. The hourly variation of thermal equivalent of electrical efficiency is been shown in same figure and it ranges between 26.6 and 30.48%. Similar calculations are done for glass-to-glass air collector and by using the data of Table 2 the parameters discussed above are calculated and the results are compared with the results of glass-to-tedlar PV/T air collector and discussed below.

Fig. 7(a) shows hourly variation of the back surface, solar cell and outlet air temperatures for both glass-to-glass and glass-to-tedlar PV/T air collector. The back surface temperature for glass-to-tedlar varies from a minimum value of 43.6 °C at 8 am to a maximum value of 68 °C at 12 pm where as for glass-to-glass PV/T air collector it varies from a minimum value of 44 °C at 8 am and 5 pm and a maximum value of 71 °C at 12 pm. It is clear from the graph that back surface temperature is higher in glass-to-glass air collector than in glass-to-tedlar. It is because of more radiations transmitted from glass get absorbed on the blackened surface. The solar cell temperature is almost same for both cases and ranges between a minimum value of 45 °C at 8 am and 5 pm to a maximum value of 70 °C at 12 pm. It is due to the fact that heating of top surface is not affected by the blackened surface attached in the air duct of glass-to-glass air collector. The outlet air temperature ranges between a minimum value of 33 °C at 8 am and a maximum value of 46 °C at 1 pm and it is slightly higher in glass-to-glass air collector due to the fact that more thermal energy is available on the back surface of glass-to-glass air collector. This effect would be more significant for lower duct air velocities.

Fig. 7(b) shows hourly variation of the electrical, thermal and overall thermal efficiencies for both glass-to-glass and glass-to-tedlar PV/T air collector. The electrical efficiency in both cases ranges between 9.5–11% through out the day. This might be because of the fact that the heat (thermal energy) removal from the back surfaces in both cases is faster then the heat absorbed by the same at a given time. The thermal equivalent of electrical efficiency for both cases is same and ranges between 26.4–30.5%. For glass-to-glass PV/T air collector thermal efficiency ranges between 15.7–18.3% and it is 13.4–16.5%

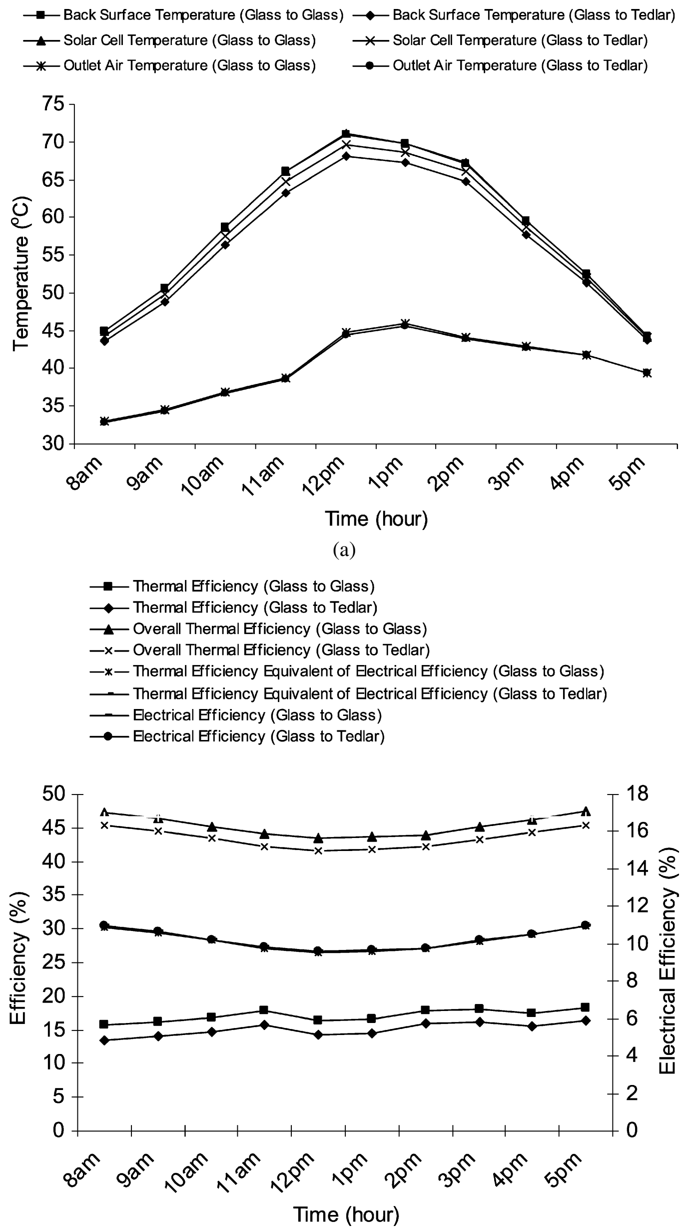

Fig. 7. (a) Hourly variation of back surface, solar cell and outlet air temperature for both glass-to-glass and glass-to-tedlar hybrid PV/T air collector. (b) Hourly variation of thermal, electrical and overall thermal efficiencies for both glass-to-glass and glass-to-tedlar hybrid PV/T air collector.

for glass-to-tedlar case. It is more in glass-to-glass PV/T air collector than in glass-to-tedlar because outlet air temperature is slightly higher in the former case.

The overall thermal efficiency is of the order of 43.4–47.4% for glass-to-glass and 41.6–45.4% for glass-to-tedlar case. It is significantly higher in case of glass-to-glass than in the glass-to-tedlar air collector. This is due to the fact that thermal efficiency is more in case of glass-to-glass due to more thermal energy extraction by duct air from black surface.

Fig. 8(a) shows the variation of overall thermal efficiency with the length of the collector (keeping velocity of duct air constant, $v = 1.6$ m/s). The overall thermal efficiency ranges

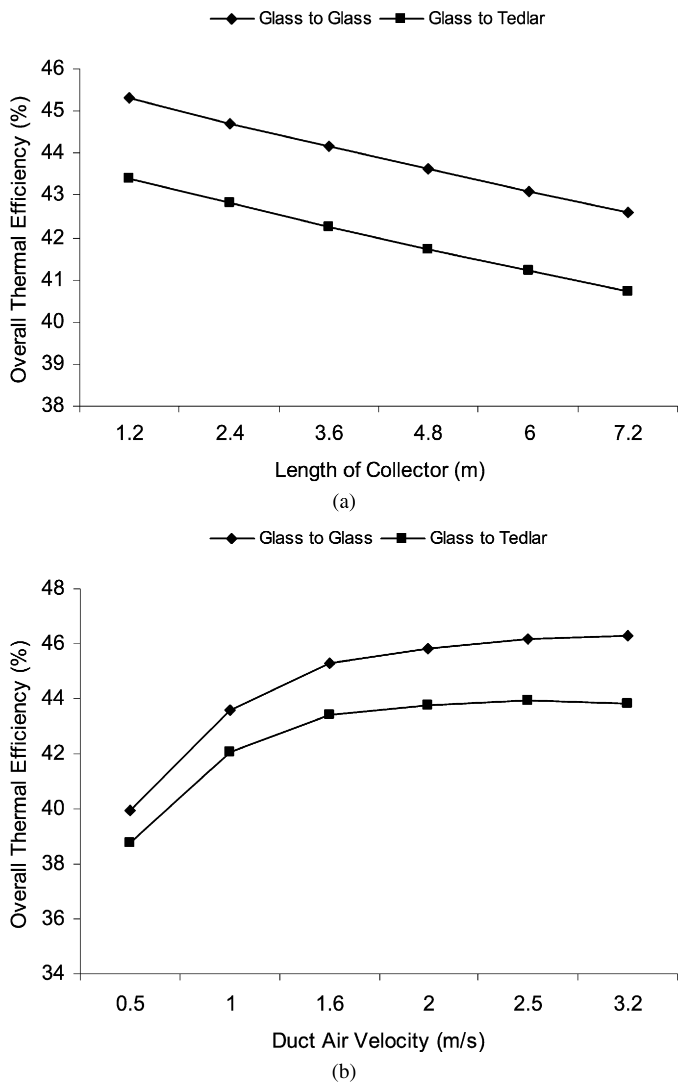

Fig. 8. (a) Variation of overall thermal efficiency with the length of the collector. (b) Variation of overall thermal efficiency for different duct air velocities.

between a maximum value of 45.3% at 1.2 m and a minimum value of 42.61% at 7.2 m for glass-to-glass case and it ranges between a maximum value of 43.41% at 1.2 m and a minimum value of 40.71% at 7.2 m duct length for glass-to-tedlar case. It decreases with increase in the length of air duct because of less thermal energy extraction from the back surface.

Fig. 8(b) shows the variation of overall thermal efficiency with the air duct velocity (keeping the length of air collector constant, $L = 1.2$ m). The overall thermal efficiency ranges between a minimum value of 39.93% at 0.5 m/s and a maximum value of 46.28% at 3.2 m/s for glass-to-glass case and it ranges between a minimum value of 38.79% at 0.5 m/s and a maximum value of 43.85% at 3.2 m/s duct air velocity for glass-to-tedlar case. It increases initially with increase in duct air velocity. This is due to the fact that more air passes through the air duct extracts more thermal energy. However, at higher air duct velocities the time of contact of air with the back surface reduces causing less heat removal from the back surface and hence, the overall thermal efficiency gets constant at higher duct air velocities.

6. Conclusions

This study has dealt with performance evaluation of a hybrid photovoltaic thermal (PV/T) air collector system. The two types of photovoltaic (PV) modules namely PV module with glass-to-tedlar and glass-to-glass are considered for comparison purpose. From the study, the following conclusions can be drawn:

- Back surface temperature is more in glass-to-glass PV/T air collector than in glass to tedlar PV/T air collector.
- Glass-to-glass PV/T air collector gives better results in terms of the thermal efficiency as compared to glass-to-tedlar PV/T air collector.
- Overall thermal efficiency of glass-to-glass PV/T air collector is more as compared to glass-to-tedlar PV/T air collector.
- Overall thermal efficiency decreases with increase in length of the duct in both cases.
- Overall thermal efficiency increases with the increase in the velocity of duct air primarily. After that, it saturates.

Further, for future work we will include the dynamic effect of weather on the cell performance as it may affect the performance of large scale photovoltaic/thermal setups.

Acknowledgements

The authors acknowledge the support provided by Indian Institute of Technology-Delhi in India and the Natural Sciences and Engineering Research Council in Canada.

References

[1] A.D. Jones, C.P. Underwood, A thermal model for photovoltaic systems, Solar Energy 70 (4) (2001) 349–359.
[2] A.K. Bhargava, H.P. Garg, R.K. Agarwall, Study of a hybrid solar system–solar air heater combined with solar cells, Energy Conversion and Management 31 (5) (1991) 471–479.
[3] A. Tiwari, M.S. Sodha, A. Chandra, J.C. Joshi, Performance evaluation of photovoltaic thermal solar air collector for composite climate of India, Solar Energy Materials and Cells 90 (2) (2006) 175–189.
[4] N. Odeh, T. Grassie, D. Henderson, T. Muneer, Modelling of flow rate in a photovoltaic-driven roof slate-based solar ventilation air pre heating system, Energy Conversion Management 47 (7–8) (2006) 909–925.
[5] Y. Vorobiev, J. Gonzalez-Hernandez, P. Vorobiev, L. Bulat, Thermal-photovoltaic hybrid system for efficient solar energy conversion, Solar Energy 80 (2) (2006) 170–176.
[6] B.P. Cartmell, N.J. Shankland, D. Fiala, V. Hanby, A multi-operational ventilated photovoltaic and solar air collector: application, simulation and initial monitoring feedback, Solar Energy 76 (2004) 45–53.
[7] A.A. Hegazy, Comparative study of the performance of four photovoltaic/thermal solar air collectors, Energy Conversion Management 41 (8) (2000) 861–881.
[8] D. Infield, L. Mei, U. Eicker, Thermal Performance estimation of ventilated PV facades, Solar Energy 76 (1–3) (2004) 93–98.
[9] Y. Tripanagnostopoulos, T.H. Nousia, M. Souliotis, P. Yianoulis, Hybrid photovoltaic/thermal solar system, Solar Energy 72 (3) (2002) 217–234.

[10] J. Prakash, Transient analysis of a photovoltaic-thermal solar collector for co-generation of electricity and hot air/water, Energy Conversion Management 35 (1994) 967–972.
[11] A. Tiwari, M.S. Sodha, Performance evaluation of a solar PV/T system: An experimental validation, Solar Energy 80 (7) (2006) 751–759.
[12] B. Sandnes, J. Rekstad, A photovoltaic/thermal (PV/T) collector with a polymer absorber plate: Experimental study and analytic model, Solar Energy 72 (1) (2002) 63–73.
[13] R. Zakharchenko, L. Licea-Jime'nez, S.A. Pe'rez-Garci'a, P. Vorobiev, U. Dehesa-Carrasco, J.F. Pe'rez-Robels, J. Gonza'lez-Herna'ndez, Y. Vorobiev, Photovoltaic solar panel for a hybrid PV/Thermal system, Solar Energy Materials and Solar Cell 82 (1–2) (2004) 253–261.
[14] T.T. Chow, Performance analysis of photovoltaic-thermal collector by explicit dynamic model, Solar Energy 75 (2003) 143–152.
[15] H.P. Garg, R.K. Agarwall, J.C. Joshi, Experimental study on a hybrid photovoltaic thermal solar water heater and its performance prediction, Energy Conversion and Management 35 (1994) 621–633.
[16] S.A. Kalogirou, Use of TRYNSYS for modeling and simulation of a hybrid PV-thermal solar system for Cyprus, Renewable Energy 23 (2001) 247–260.
[17] H.A. Zondag, D.W. de Vries, W.G.J. van Helden, R.J.C. van Zolingen, A.A. van Steenhoven, The thermal and electrical yield of a PV-thermal collector, Solar Energy 72 (2) (2002) 113–128.
[18] B.J. Huang, T.H. Lin, W.C. Hung, F.S. Sun, Performance evaluation of solar photovoltaic/thermal systems, Solar Energy 70 (5) (2001) 443–448.
[19] K. Sopian, H.T. Liu, S. Kakac, T.N. Veziroglu, Performance of a double pass photovoltaic thermal solar collector suitable for solar drying systems, Energy Conversion and Management 41 (4) (2000) 353–365.
[20] S.J. Coventry, Performance of a concentrating photovoltaic/thermal solar collector, Solar Energy 78 (2) (2005) 211–222.
[21] A.D. Sahin, I. Dincer, M.A. Rosen, Thermodynamic analysis of solar photovoltaic cell systems, Solar Energy Materials and Solar Cells 91 (2–3) (2007) 153–159.
[22] Photovoltaic systems Technology Fundamentals published in Renewable Energy World (2004) 81–84, http://www.volkerquaschning.de/articles/fundamentals3/index_e.html.
[23] Siemens Solar Panels direct from Bullnet, http://www.siemenssolar.co.uk/.
[24] A.S. Joshi, Evaluation of cloudiness/haziness factor and it's application for photovoltaic thermal (PV/T) system for Indian climatic conditions, PhD thesis, IIT Delhi, 2006.
[25] A Strategy for Growth of Electrical Energy in India, Document 10, Department of Atomic Energy, Government of India, http://www.dae.gov.in/publ/doc10/index.htm.